Theoretical, Structural, Vibrational, NMR, and Thermal Evidence of the Inter- versus Intramolecular Hydrogen Bonding in Oxamides and Thiooxamides

H. O. Desseyn,*,† S. P. Perlepes,‡ K. Clou,† N. Blaton,§ B. J. Van der Veken,† R. Dommisse,† and P. E. Hansen||

Department of Chemistry, University of Antwerp, RUCA, Groenenborgerlaan 171, 2020 Antwerp, Belgium, Laboratory of Inorganic Chemistry, Department of Chemistry, University of Patras, Rio-Patra, Greece, Laboratory of Analytical Chemistry & Medicinal Physicochemistry, University of Leuven, Leuven, Belgium, and Department of Live Science and Chemistry, Roskilde University, P.O. Box 260, DK-4000 Roskilde, Denmark

Received: February 26, 2004

This contribution describes the study of hydrogen bonding in secondary oxamides, monothiooxamides, and dithiooxamides by ab initio calculations, X-ray diffractions, NMR spectra, thermal analysis, and variable-temperature infrared and Raman spectroscopy. The results can all be interpreted as a function of the change in the strength and the nature of the hydrogen bonding by substituting oxygen for sulfur in the series CH_3-HNCOCONHCH$_3$, CH_3HNCSCONHCH$_3$, CH_3HNCSCSNHCH$_3$ and by changing the steric influence of the alkyl group in a series of oxamides (RHNCOCNHR; R = CH_3, C_2H_5, iC_3H_7, tC_4H_9).

Introduction

In this work, we studied the change in the character of the hydrogen bonding in two series of original compounds. The hydrogen bonding has been studied using different techniques. X-ray structures and ab initio calculations give direct information because the most reliable criterion is based on the van der Waals radii[1] and also the angle involved in the hydrogen bonding.[2] Vibrational spectroscopy has always been the main experimental method in the study of hydrogen bonding, and we obtained very valuable information from the temperature-dependent solid-state spectra,[3−5] especially when solubility problems were encountered. Concentration- and temperature-dependent NMR spectroscopy[6−23] and especially the enthalpies confirm the trend indicated by X-ray and vibrational spectroscopy between inter- and intramolecular character, as indicated by structural and vibrational spectroscopy.

The comparison of these different techniques clearly shows that infrared and Raman spectroscopy are the best techniques for these typical kinds of studies; the other techniques used in this work also give important information throughout the whole study.

The compounds under investigation are original oxamides, thiooxamides, and dithiooxamides. These molecules form an important group of ligands in coordination chemistry.[24] A remarkable characteristic of these ligands is their thermal and chemical stability and especially their dissociation constants.[25] The very important role of hydrogen bonding in these various characteristics has been extensively studied.[5,26−32]

Experimental Section

Infrared spectra were recorded on a Bruker IFS 113v Fourier transform spectrometer using a globar source, a Ge/KBr beam splitter, and a liquid-nitrogen-cooled MCT detector. Spectra at a resolution of 1 cm^{-1} were recorded using interferograms averaged over 100 scans, Happ Geuzel apodized, and Fourier transformed by applying a zero filling factor of 2.

Solid-state low-temperature infrared spectra were obtained using a cryostat consisting of a sample holder fixed to the bottom of a liquid-nitrogen container suspended in a vacuum shroud. The cryostat is optically coupled to the spectrometer using KBr windows. All solid-state samples were studied in KBr pellets.

Fourier transform Raman spectra were recorded on a Bruker IFS 66v interferometer equipped with an FT Raman FRA 106 module. The compounds were excited by the 1064-nm line of a Nd:YAG laser operating at 200 mW. For each spectrum, 1000 scans were recorded and averaged. Low-temperature Raman spectra were recorded in a Miller−Harney cell using a SPEX 1403 double monochromator. The compounds were excited by a Spectra Physics model 2020 Ar^+ laser. The spectra were recorded with a spectral slit width of 4 cm^{-1}.

Enthalpies were measured on a TA instrument DSC 2920 equipped with an RCS cooling system and on an SDT 2960 simultaneous DSC−TGA instrument. The experiments were performed under a dry nitrogen atmosphere (50 mL min^{-1}), and the heating rate was 1 K min^{-1}. The thioamides under investigation are known to be good complexing agents with very soft acids. Because zero-valent metals in the standard DSC all are very soft acids, they tend to form complexes, especially with the thioamides, resulting in a deterioration of the cell, causing considerable changes in the cell constant. Therefore, the recently developed DSC−TGA upgrade for the SDT made of corrosion-resistant material was used in the present measurements.

The NMR spectra were recorded on a Varian 400-MHz spectrometer; the chemical shifts are given in ppm. DMSO-*d*6 was used as a solvent, and TMS was used as an internal standard.

X-ray Crystallography. Crystals were mounted on a glass fiber using epoxy glue. A preliminary examination and data collection were performed on a computer-controlled four-circle

* Corresponding author. E-mail: jozef.janssens@ua.ac.be.
† University of Antwerp.
‡ University of Patras.
§ University of Leuven.
|| Roskilde University.

10.1021/jp0401776 CCC: $27.50
Published on Web 05/21/2004

TABLE 1: Crystallographic Data for Compounds DMMTO, DMDTO, DEO, DiPO, and DtBO

parameter	DMMTO	DMDTO	DEO	DiPO	DtBO
chemical formula	$C_4H_8N_2OS$	$C_4H_8N_2S_2$	$C_6H_{12}N_2O_2$	$C_8H_{16}N_2O_2$	$C_{10}H_{20}N_2O_2$
fw	132.18	148.24	144.18	172.23	200.28
space group	P1	$P2_1/c$	$P2_1/n$	$P2_1/c$	*Pbcn*
a, Å	6.234 (2)	17.141 (5)	5.077 (1)	5.154 (1)	9.989 (3)
b, Å	6.700 (1)	4.194 (1)	10.016 (1)	9.833 (1)	11.455 (3)
c, Å	8.105 (2)	10.366 (6)	8.226 (1)	10.522 (1)	10.300 (4)
α, deg	89.18 (1)				
β, deg	80.35 (3)	107.44 (4)	97.80 (1)	101.89 (1)	
γ, deg	80.05 (1)				
V, Å^3	328.7 (1)	710.9 (5)	414.5 (1)	521.9 (1)	1178.6 (6)
Z	2	4	2	2	8
T, K	293 (2)	293 (2)	293 (2)	293 (2)	293 (2)
λ, Å	1.54178	0.71073	1.54178	1.54184	1.54178
D_{calcd}	1.336	1.385	1.155	1.096	1.129
μ, mm^{-1}	3.642	0.649	0.724	0.645	0.633
R1[a]	0.0413	0.0347	0.0591	0.0761	0.0443
wR2[b]	0.1213	0.0888	0.1618	0.2076	0.1152

[a] $R1 = \Sigma(|Fo|-|Fc|)/\Sigma(|Fo|)$. [b] $wR2 = \{\Sigma[w(Fo^2 - Fc^2)^2]/\Sigma[w(Fo^2)^2]\}^{1/2}$.

diffractometer with graphite monochromator (Siemens P4 using Cu Kα or Stoe Stadi4 using Mo Kα radiation) at room temperature.

Omega scans for several intense reflections were used as a criterion for acceptable crystal quality. Three standard reflections monitored every 100 reflections indicated crystal stability. A semiempirical absorption correction was employed.[33] The structures were solved by direct methods.[34]

Further crystallographic details are given briefly as follows. Compound DMMTO: $2\theta_{(max)} = 137.6°$ (Cu Kα radiation), reflections collected/unique 1497/1169 ($R_{int} = 0.0567$), 76 parameters refined, $(\Delta\rho)_{max}/(\Delta\rho)_{min} = 0.204/-0.202$e Å^{-3}. Compound DMDTO: $2\theta_{(max)} = 50.0°$ (Mo Kα radiation), reflections collected/unique 4554/1245 ($R_{int} = 0.0482$), 76 parameters refined, $(\Delta\rho)_{max}/(\Delta\rho)_{min} = 0.220/-0.188$ e Å^{-3}. Compound DEO: $2\theta_{(max)} = 137.8°$ (Cu Kα radiation), reflections collected/unique 1116/724 ($R_{int} = 0.0328$), 56 parameters refined, $(\Delta\rho)_{max}/(\Delta\rho)_{min} = 0.184/-0.153$e Å^{-3}. Compound DIPO: $2\theta_{(max)} = 137.9°$ (Cu Kα radiation), reflections collected/unique 1402/918 ($R_{int} = 0.0280$), 61 parameters refined, $(\Delta\rho)_{max}/(\Delta\rho)_{min} = 0.298/-0.241$e Å^{-3}. Compound DTBO: $2\theta_{(max)} = 138.5°$ (Cu Kα radiation), reflections collected/unique 1414/1028 ($R_{int} = 0.0430$), 71 parameters refined, $(\Delta\rho)_{max}/(\Delta\rho)_{min} = 0.186/-0.189$e Å^{-3}.

For all structures, all non-hydrogen atoms were refined anisotropically. Most hydrogen atoms were geometrically idealized and allowed to ride on their parent atoms (O−H = 0.82, C−H = 0.96, and N−H = 0.86 Å). The isotropic displacement parameters of all hydrogen atoms were assigned to be 1.3 times those of their parent atoms.[35]

The crystal structure of $CH_3HNCOCONHCH_3$ has been described.[36] For the other compounds $CH_3HNCOCSNHCH_3$ (DMMTO), $CH_3HNCSCSNHCH_3$ (DMDTO), $C_2H_5HNCOCONHC_2H_5$ (DEO), $iC_3H_7HNCOCONHiC_3H_7$ (DiPO), and $tC_4H_9HNCOCONHtC_4H_9$ (DtBO), we gathered the crystallographic data in Table 1.

Synthesis of the Compounds. RHNCOCONHR derivatives were synthesized by reacting $CH_3OOCCOOCH_3$ with 2.2 equiv of RNH_2 in ethanol under reflux for $^1/_2$ h. The colorless compounds were purified by recrystallization from ethanol.

RHNCSCSNHR derivatives were synthesized by reacting dithiooxamide ($H_2NCSCSNH_2$) with 2.2 equiv of RNH_2 in ethanol under reflux for 2 h. The colored compounds were purified by recrystallization from ethanol.

RHNCSCONHR derivatives have been prepared according to the following reactions:

$$H_2NCOCOOC_2H_5 \text{ (Fluka 619083)} \xrightarrow[T\uparrow]{P_2O_5} NCCOOC_2H_5$$

$$NCCOOC_2H_5 \xrightarrow[\text{toluene}]{H_2S} H_2NCSCOOC_2H_5$$

$$H_2NCSCOOC_2H_5 + 2.2RNH_2 \xrightarrow[\text{toluene}]{\text{reflux}} RHNCOCSNHR$$

The pale-yellow compounds were purified by recrystallization from ethanol.

The single crystals for the X-ray diffraction experiments were prepared by the double-layer method (i.e., by adding hexane to a solution of the compound in CH_2Cl_2).

Computational Details. Density functional theory calculations were performed using Gaussian 98.[37] For all calculations, Becke's three-parameter exchange functional[38] was used in combination with the Lee−Yang−Parr correlation functional,[39] and the B3LYP/6 31++G** basis set was used. To reduce the errors arising from the numerical integration, the "fine-grid" option, corresponding to roughly 7000 grid points per atom, was used for all calculations. To obtain information about multimers ($n = 2$, 3, 4, 5, and 6) the equilibrium geometry was calculated without structural restrictions. For all equilibrium geometries, the vibrational frequencies and the intensities were calculated using harmonic force fields.

Results and Discussion

1. X-ray Study. The most reliable criterion of hydrogen bond formation is that based on the van der Waals radii. The van der Waals radii of the atoms that are possibly engaged are 1.55 (N), 1.52 (O), and 1.80 Å (S).[40] Thus, for N···O and N···S distances shorter than 3.07 and 3.35 Å, respectively, the presence of a hydrogen bond must be considered. We can also consider H···A distances with the van der Waals radius of the H atom ranging from 1.00 to 1.20 Å,[40] resulting in hydrogen bonds for H···O and H···S distances between 2.52 and 2.72 Å and 2.80 and 3.00 Å, respectively.

Because of the uncertainties in the hydrogen positions, we will analyze the hydrogen bonds in terms of the N···O and N···S inter- and intramolecular distances, although the H···O and H···S distances shown in the Tables generally confirm the results obtained from the N···O and N···S distances.

Table 2 compares relevant experimental and calculated (monomer) distances and angles involved in the hydrogen bonding in DMO, DMMTO, and DMDTO.

DMO appears in the trans-planar configuration, exhibiting the typical intermolecular peptide hydrogen bonding as given in Figure 1. Both the inter- and intramolecular N···O distances (2.720 and 2.860 Å) are shorter than the van der Waals radius (3.07 Å), clearly indicating the bifurcated hydrogen bonding in these molecules.

DMDTO molecules also appear in the trans-planar configuration as given in Figure 2. The molecule exhibits two slightly different CN and CS distances per molecule; this phenomenon has already been described in the structural study of the hydroxyethyl derivative.[41] The inter- and intramolecular N···S distances (average) of 2.943 and 3.484 Å are very different, and the intermolecular N···S distance is even considerably greater than the sum of the van der Waals radii (3.35 Å), leading

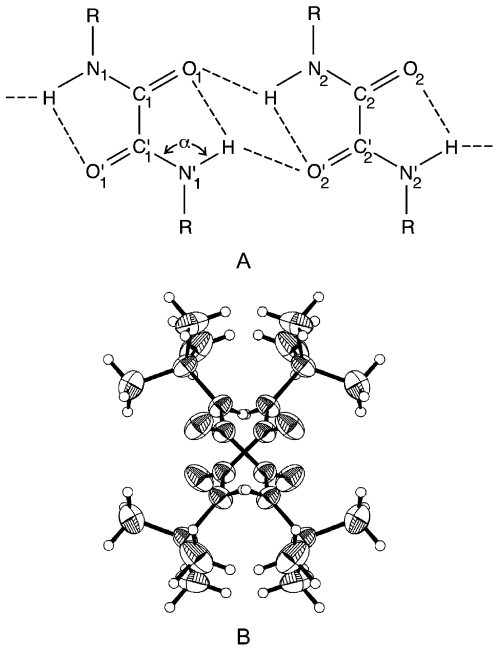

Figure 1. (A) Infinite chains of hydrogen-bonded oxamide units in the crystal structures of DMO (R = CH_3), DEO (R = C_2H_5), and DiPO (R = iC_3H_7). (B) Packing of the molecules in the crystal structure of DtBO.

TABLE 2: Inter- and Intramolecular Distances (Å) and Angles in DMO, DMMTO, and DMDTO Involved in Hydrogen Bonding

		DMO	DMMTO	DMDTO
CO	calcd	1.230	1.233	
	exptl	1.226	1.218	
CS	calcd		1.670	1.679
	exptl		1.663	1.673/1.665
CN_{amide}	calcd	1.347	1.343	
	exptl	1.328	1.317	
$CN_{thioamide}$	calcd		1.330	1.329
	exptl		1.306	1.458/1.309
$O\cdots N_{intra}$	calcd	2.695	2.602	
	exptl	2.720	2.627	
$S\cdots N_{intra}$	calcd		3.059	2.971
	exptl		3.020	2.945/2.942
$O\cdots N_{inter}$	exptl	2.860	2.860	
$S\cdots N_{inter}$	exptl		3.433	3.479/3.488
∠NCO	calcd	126.67	125.63	
	exptl	125.26	124.42	
∠NCS	calcd		125.82	124.11
	exptl		125.19	124.52/124.52
∠CCO	calcd	121.76	119.49	
	exptl	121.19	119.66	
∠CCS	calcd		124.55	122.48
	exptl		122.92	121.73/121.13
∠NHO	calcd	108.22	111.18	
	exptl	112.88	114.22	
∠NHS	calcd		114.61	117.65
	exptl		114.72	117.55/117.96
$H\cdots O_{inter}$	exptl	2.163	2.078	
$H\cdots O_{intra}$	calcd	2.213	2.214	
	exptl	2.309	2.054	
$H\cdots S_{inter}$	exptl		2.802	>3.50
$H\cdots S_{intra}$	calcd		2.493	2.355
	exptl		2.559	2.444

to the conclusion that in DMDTO we can mainly consider strong intramolecular hydrogen bonding, although the packing of the molecules as given in Figure 2 suggests some intermolecular interaction.

DMMTO molecules also exhibit a planar-trans configuration (Figure 3). From the inter- and intramolecular alternating

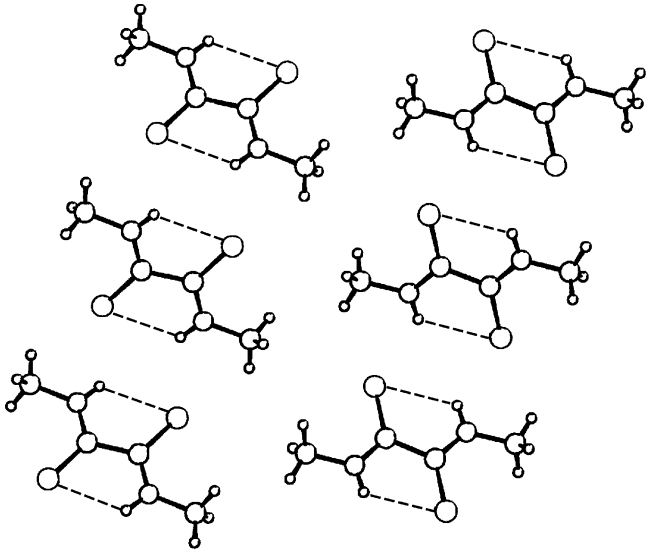

Figure 2. Packing of the molecules in the crystalline phase of DMDTO.

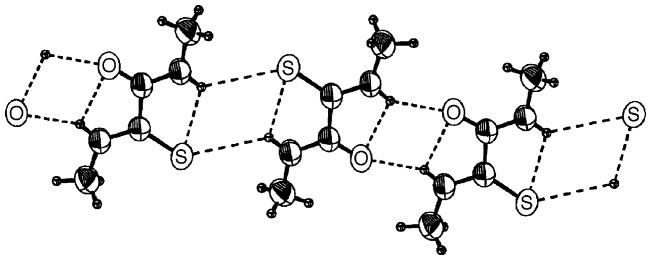

Figure 3. Hydrogen bonding in the crystalline phase of DMMTO.

N···O and N···S distances, we can conclude that bifurcated

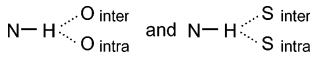

exist.

Although the intermolecular S···N distance (3.433 Å) is longer than the sum of the van der Waals radii, it is shorter than the S···N intermolecular distance observed for DMDTO (3.388 Å). For DMMTO, we can conclude that the hydrogen bonding for the amide hydrogen obtains more intramolecular character compared to DMO and that the thioamide hydrogen shows more intermolecular character compared to DMDTO.

The influence of the cooperative effect in hydrogen-bonded oligomers of DMO on the strength of the hydrogen bonding and the effect on the CO and CN distances was studied using DFT calculations on the monomer ($x = 1$), trimer ($x = 3$), and pentamer ($x = 5$). The main results have been collected in Table 3. It can be seen that the pentamer exhibits longer CO and NH but shorter CN bond lengths compared with those of the monomer, suggesting stronger intermolecular hydrogen bonds with the increasing number of monomers in the chain. This increasing intermolecular strenght is also demonstrated by the average hydrogen bond energy defined as

$$\frac{E_{(\mathrm{DMO})x} - xE_{\mathrm{DMO}}}{x - 1} \qquad (x = \text{number of molecules})$$

This energy increases from 22.4 kJ mol^{-1} in the dimer to 23.0 kJ mol^{-1} in the pentamer. For *N*-methylacetamide, exhibiting only intermolecular hydrogen bonds, this energy changes from 31.8 to approximate 39 kJ mol^{-1} for the pentamer.[4] Thus, the intermolecular interactions in DMO are about 30% weaker

TABLE 3: Cooperative Effect in DMO[a]

		monomer	trimer[d]	pentamer[d]	solid state 25 °C	solid state −196 °C
N−H[b]		1.014	1.019	1.019		
νNH		3400	3335	3328	3312	3299
CN[c]		1.347	1.340	1.337		
νCN	amide II	1518	1537	1538	1558	1560
	amide III	1215	1254	1259		
CO[b]		1.230	1.235	1.238	1.293	1.295
νCO	amide I	1691	1684	1681	1660	1658
$O\cdots H_{inter}$[c]			1.971	1.956		
$O\cdots H_{intra}$[b]		2.200	2.299	2.379		
$\angle OHN_{inter}$[b]			149.00	150.45		
$\angle OHN_{intra}$[c]		108.22	103.17	101.91		

[a] Distances (Å); angles and frequencies (cm^{-1}) (See footnote d.) [b] Highest values in the series. [c] Lowest value in the series. [d] The frequency of the relatively most intense band from the series is given.

TABLE 4: Distances and Angles in DMO, DEO, DiPO, and DtBO Involved in Hydrogen Bonding[a]

compound		DMO[42]	DEO	DiPO	DtBO
CO	exptl	1.226	1.226	1.212	1.229
CN	exptl	1.328	1.317	1.320	1.330
$O\cdots N_{intra}$	exptl	2.720	2.704	2.699	2.683
$O\cdots N_{inter}$	exptl	2.860	2.893	2.997	3.568
$H\cdots O_{intra}$	exptl	2.309	2.286	2.403	2.250
$H\cdots O_{inter}$	exptl	2.163	2.100	2.111	2.692
νNH	calcd	3400	3400	3384	3374
$\nu NH_{dil.CH_2Cl_2}$	exptl	3412	3399	3387	3377

[a] Distances in Å; ν in cm^{-1}.

compared with those of *N*-methylacetamide. This difference must be assigned to the considerable intramolecular interaction in DMO.

Table 3 also lists the vibrational frequencies for some characteristic amide fundamentals, calculated for the monomer and multimers, and the experimental data of the solid-state spectra at different temperatures.

These frequency shifts on passing from the monomer (gas phase) to the multimers to the solid state at room temperature ($x = \infty$) and the shift observed at lower temperature can be well explained by considering stronger intermolecular hydrogen bonding in this series, which is due to the cooperative effect and the fact that the change in temperature in the solid state causes a change in the intermolecular distances and consequently a change in the donor−acceptor strength, resulting in stronger intermolecular interactions at lower temperatures.[42,43]

Table 4 compares relevant distances concerning hydrogen bonding for oxamides exhibiting different CH_3 groups on the α carbon of the alkyl group.

The CO and CN bond lengths are all comparable; in both cases (inter- and intramolecular hydrogen bonds), we expect longer CO and shorter CN bond lengths due to the resonance-assisted intra- and intermolecular hydrogen bonding. From the changes in the inter- and intramolecular N···O distances, we can clearly conclude that the intramolecular character increases with the steric hindrance, which is caused by the number of CH_3 groups on the α carbon of the alkyl groups. Furthermore, it is very clear that the hydrogen bonding in the tC_4H_9 derivative is practically purely intramolecular because the intermolecular N···O distance is greater than 3.568 Å. The fact that the tC_4H_9 derivative does not exhibit the typical linear peptide structure is caused by this pure intramolecular character in the hydrogen bonding (Figure 1B).

Table 4 also gives the theoretical νNH in the gas phase and the νNH frequencies in very dilute CH_2Cl_2. In both series, we observe a decreasing νNH frequency, indicating the increasing intramolecular character.

TABLE 5: Comparison of Some Fundamentals Influenced by Hydrogen Bonding in DMO, DMMTO, and DMDTO[a]

		DMO	DMMTO O	DMMTO S			DMDTO
νNH exptl	25 °C	3312	3303	3247			3180
	$\Delta\nu$[b]	13	4	3			0
πNH	25 °C	765	817	681	πNH	25 °C	712
	$\Delta\nu$[b]	20	4	7			0
amide I	25 °C	1660	1677	1535	νCN	25 °C	1538
	−190 °C	1657	1677	1537		−190 °C	1538
amide II	25 °C	1533	1560				
	−190 °C	1537	1560				
amide III	25 °C	1237	1240				
	−190 °C	1240	1240				

	$\nu NH_{dil.\ CH_2Cl_2}$	νNH_{solid} (25 °C)	$\Delta\nu$
DMO	3412	3312	100
DMMTO (O)	3341	3303	38
(S)	3300 sh	3247	(53)
DMDTO	3192	3180	12

[a] IR band in cm^{-1}. [b] $\Delta\nu = \nu(298\ K) - \nu(77\ K)$.

2. Vibrational Spectra. Table 5 gives the νNH fundamentals in the solid state at different temperatures and in dilute CH_2Cl_2 solutions and some other significant fundamentals in the solid state of DMO, DMMTO, and DMDTO. The νNH in the solid state of secondary amides and thioamides depends on the acidity (thioamides are more acidic than amides and the νNH modes appear at lower frequencies), the mass of the alkyl substituent, and the geometry of the molecule, so from the position of the νNH in the solid state, no conclusions can be made. However, the $\Delta\nu$ values (i.e., the difference between the νNH in the solid state and the νNH of the compound in dilute CH_2Cl_2) give a direct indication of the strength of the intermolecular hydrogen bonding. From these $\Delta\nu$ values, given in Table 5, we can learn that DMO exhibits intermolecular hydrogen bonds and that intermolecular hydrogen bonding in DMDTO is nonexistent because the small $\Delta\nu$ value (12 cm^{-1}) must be ascribed to the interactions of the molecules in the solid state.[44] The amide νNH mode shows less intermolecular association in DMMTO, but this intermolecular character becomes more pronounced for the thioamide νNH mode in DMMTO compared with that in DMDTO.

This increased intramolecular character of the amide and the increased intermolecular character of the thioamide group in DMMTO are also confirmed in the solid-state spectra at different temperatures. νNH of DMO shifts about 13 cm^{-1} to lower frequency, and πNH shifts 20 cm^{-1} to higher frequency, which is indicative of intermolecular hydrogen bonding. The zero shift of the νNH and πNH in DMDTO clearly indicate pure intramolecular hydrogen bonding. The shift observed for DMMTO again indicates more intramolecular character for the amide and less intramolecular character for the thioamide hydrogen bonding.

The shift to lower frequency of the amide I band (mainly νCO) and the shift to higher frequency of the amide II and amide III band (δNH + νCN) by lower temperature confirm the intermolecular character in DMO. The zero shift of the νCN in the thioamide group indicates pure intramolecular character in DMDTO.

Again for DMMTO we observe smaller frequency shifts for the amide fundamentals and a slight shift of the νCN of the thioamide function, confirming more intramolecular character for the amide group and more intermolecular character for the thioamide group interaction in DMMTO compared with that in DMO and DMDTO, respectively.

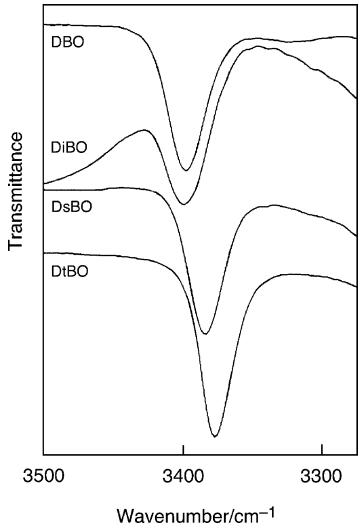

Figure 4. νNH modes of different butyloxamides in dilute CH_2Cl_2.

TABLE 6: Comparison of νNH Modes in the Solid State and in Dilute CH_2Cl_2 Solutions (cm^{-1}) of Some Oxamides (cm^{-1})

compound		$\nu NH_{dil.\ CH_2Cl_2}$	νNH_{solid} (25 °C)	$\Delta\nu$
MA	methylacetamide	3461	3304	157
DMO	($CH_3HNCOCONHCH_3$)	3412	3312	100
DEO	($C_2H_5HNCOCONHC_2H_5$)	3399	3304	95
DiPO	($iC_3H_7HNCOCONHiC_3H_7$)	3387	3298	89
DtBO	($tC_4H_9HNCOCONHtC_4H_9$)	3377	3338	39
DBO	($C_4H_9HNCOCONHC_4H_9$)	3397	3299	98
DiBO	($iC_4H_9HNCOCONHiC_4H_9$)	3404	3307	97
DsBO	($sC_4H_9HNCOCONHsC_4H_9$)	3384	3295	89

	I.R. νNH			Raman		
	25 °C	−120 °C	$\Delta\nu$	25 °C	−196 °C	$\Delta\nu$
DMO	3312	3299	13	3319	3308	11
DEO	3304	3289	15	3303	3292	11
DiPO	3298	3291	7	3299	3295	4
DtBO	3338	3336	2	3334	3332	2
MA	3304	3284	20	3300	3282	18

Table 6 gives the $\Delta\nu$ values in the solid-state infrared and Raman spectra (Bu and Ag) and the $\Delta\nu$ differences between the solid-state spectra at 21 °C and the νNH in very dilute CH_2Cl_2 for the oxamides. For methylacetamide (MA), exhibiting only intermolecular hydrogen bonds, we observed considerable $\Delta\nu$ values from the solid-state spectra at different temperatures as well as from the difference between the νNH in the solid state and the νNH in dilute CH_2Cl_2. Consequently, these shifts are a measure of the intermolecular forces, and they decrease with increasing steric hindrance.

Because the νNH of secondary amides also depends on the mass of the alkyl group, we studied the four butyl groups, exhibiting the same mass but different in their steric hindrance. Figure 4 nicely shows the influence of the steric effect on the free νNH modes.

3. NMR Spectra. DMO, DMMTO, and DMDTO were dissolved in dioxane-d_8 containing 1.8% D_2O, and the exchange rate was determined by integrating the N−H signal intensity. The observed half-life times are given in Table 7.

The hydrogen atoms of the thioamide groups appear to exchange much faster because of the more acidic character. These results also confirm the structural and vibrational results (i.e., the amide proton in DMMTO has stronger intramolecular character compared with that in DMO, and the thioamide proton has stronger intermolecular character compared with that in DMDTO).

TABLE 7: NMR Data[a]

product		$\Delta\delta/\Delta T$ DMSO-$d6$	$t_{1/2}$ 1.8 % D_2O in dioxane	$\Delta\delta/\Delta C$ ($CDCl_3$)
DMDTO		2.0	<1	0
DMMTO	CSNH	3.6	2	0.44
	CONH	2.7	452	0.11
DMO		4.4	143	1.01
DEO		4.4	[a]	[a]
DiPO		4.4	[a]	[a]
DtBO		2.4	[a]	[a]

[a] not soluble

[a] $\Delta\delta/\delta T$ (ppm/K), $t_{1/2}$ (min), and $\Delta\delta/\Delta C$ (ppm/M). [b] Not soluble.

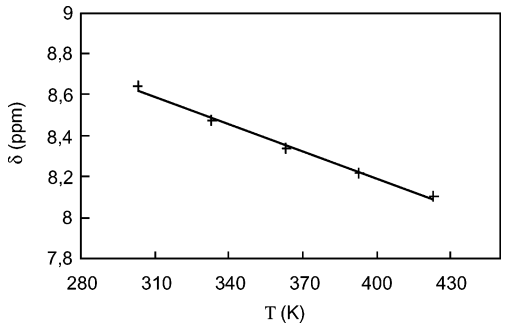

Figure 5. δ as a function of T(K) for the amide protons in DMO.

Concentration studies from 0.005 to 1 M (0.15 M for DMO) were carried out in $CDCl_3$ to minimize solvent interactions. The results were expressed as a $\Delta\delta/\Delta C$ value and are also listed in Table 7.

A comparison of the $\Delta\delta/\Delta C$ values of the amide proton in DMO and DMMTO shows that the former one has more pronounced intermolecular interaction. The extremely low value of $\Delta\delta/\Delta C$ for the thioamide hydrogen in DMDTO, however, results from the strong intramolecular interaction in this compound.

Temperature coefficients ($\Delta\delta/\Delta T$) have been used routinely in amides and thioamides to gauge intramolecular hydrogen bonding.[8,11,17,19] The $\Delta\delta/\Delta T$ values are linear within the experimental error (±0.03 ppm), as can be seen from Figure 5 for the amide protons in DMO.

$\Delta\delta/\Delta T$ values in DMSO are situated between -4×10^{-3} and -12×10^{-3} ppm/K for intermolecular systems and between -1×10^{-3} and 2×10^{-3} for strong intramolecular hydrogen bonding.[14,32,45−47]

The spectra were recorded at 30, 60, 90, 120 and 150 °C (-3×10^{-3} ppm/K is given in Table 7 as 3 ppm/K).

The temperature coefficients clearly show intramolecular hydrogen bonding in DMDTO and intermolecular

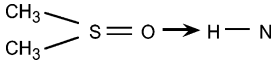

interactions in DMO.

All three $\Delta\delta/\Delta T$, $t_{1/2}$, and $\Delta\delta/\Delta C$ values indicate more intramolecular character for the amide group and less intramolecular character for the thioamide group in DMMTO than in DMO and DMDTO.

By comparing the oxamides, we can distinguish between only DtBO and DMO, DEO and DiPO. The intramolecular association observed from the structural and vibrational data is too weak

TABLE 8: DSC Values for Some Amides and Thiomides

product		$\Delta_{total}H^*$	α	no. of intermolecular H bonds
$(CH_3)_2NCOCON(CH_3)_2$	I	70		0
$(CH_3)_2NCSCON(CH_3)_2$	II	75		0
$(CH_3)_2NCSCSN(CH_3)_2$	III	82		0
$(C_2H_5)_2NCOCON(C_2H_5)_2$	IV	80		0
$(C_3H_7)_2COCON(C_3H_7)_2$	V	88		0
$H_2NCOCONH_2$	VI	109		4
$CH_3NHCOCONHCH_3$	VII	83	0	2
$C_2H_5NHCOCONHC_2H_5$	VIII	94	1	2
$C_3H_7NHCOCONHC_3H_7$	IX	105	1	2
$C_4H_9NHCOCONHC_4H_9$	X	123	1	2
$iC_4H_9NHCOCONHiC_4H_9$	XI	118	1	2
$sC_4H_9NHCOCONHsC_4H_9$	XII	112	2	2
$tC_4H_9NHCOCONHtC_4H_9$	XIII	97	3	2
$CH_3HNCSCSNHCH_3$	XIV	79		0
$CH_3HNCOCSNHCH_3$	XV	82		2
$HOC_2H_4HNCOCONHC_2H_4OH$	XVI	146 (cfr. propyl)		4
$HOC_3H_6HNCOCONHC_3H_6OH$	XVII	152		4
$HOC_4H_8HNCOCONHC_4H_8OH$	XVIII	166		4

TABLE 9: DSC and TGA Data for *N*,*N*′-Dipropyloxamide at Different Heating Rates

β °C min^{-1}	$\Delta_{total}H^*$ kJ/mol	$T(dm/dT)_{max}$ °C	residue %
0.25	91	139	3.8
0.5	92	148	4.6
1	92	146	6.8
2	91	165	8.4
10	92	192	13.7
15	95	200	15.3
20	98	203	18.8

to resist the strong interaction with the solvent (DMSO). In DtBO, however, the strong intramolecular character is confirmed.

4. DSC Measurements. Table 8 contains the DSC data ($\Delta_{total}H^*$) for different amides and thioamides. These $\Delta_{total}H^*$ values all refer to the energy involved in the change from the solid state to the gas phase. This $\Delta_{total}H^*$ can also be the sum of $\Delta_{melt}H$ and $\Delta_{vap}H$ and eventually some small contribution of Δ_{decomp}H. This $\Delta_{decomp}H$ is acceptable because the contribution is very small and also because we compare the results in a series of compounds with only the number and strength of intermolecular hydrogen bonds as variable components.

A typical example of the $\Delta_{total}H^*$ is given in Table 9, and the solid → gas phase transitions at different heating rates for *N*,*N*′-dipropyloxamide are shown in Figure 6. At very low heating rates (β values), the compound is completely sublimed before the melting point; we further clearly observe the melting and evaporation of the compound at higher β values. The residue also given in Table 9 is a direct indication of the decomposition of the compound. Therefore, $\Delta_{total}H^*$ values at a low heating rate (1 °C min^{-1}) are used in Table 8.

It is very well known that in a series of comparable compounds (comparable lattice energy) $\Delta_{total}H^*$ increases with increasing molecular mass. This is shown in the series (I, II, III) where oxygen is replaced by sulfur (Figure 7A), in the series (VII, VIII, IX, X) where the mass of the alkyl group (with $\alpha = 1$) increases, and in the series (XVI, XVII, XVIII) with increasing alkyl length in the hydroxyalkyloxamides.

By comparing the RHNCOCONHR-butyl derivatives (X, XI, XII, XIII), we clearly can see that although these compounds have the same mass the $\Delta_{total}H^*$ decreases by increasing α. This confirms the conclusion for the structural, vibrational, and NMR data that by increasing α we observe a weaker intermolecular and a stronger intramolecular interaction.

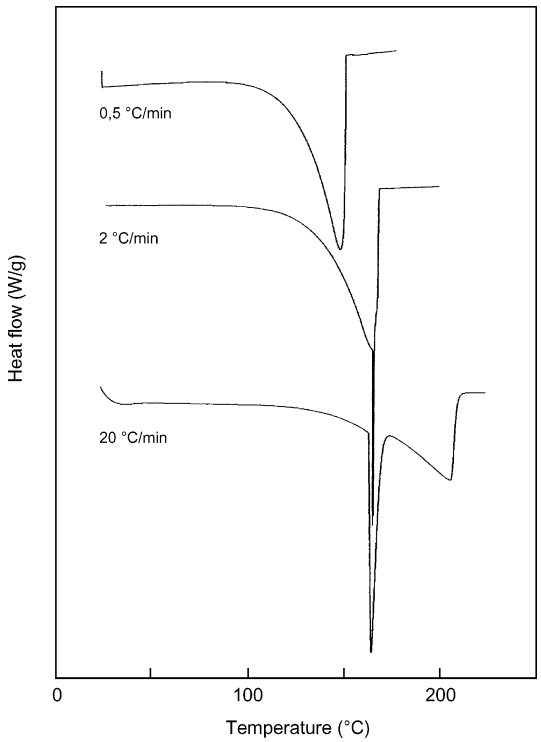

Figure 6. Solid → gas-phase transitions for DPO at different heating rates.

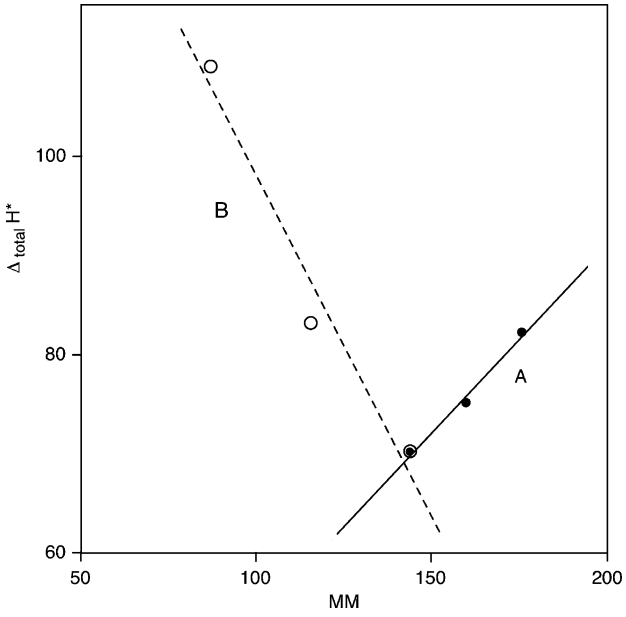

Figure 7. Relations between $\Delta_{total}H^*$ and the molecular mass in oxamides and thiooxamides.

By comparing VI, VII, and I, we see that despite the increasing mass we observed a decrease in $\Delta_{total}H^*$ values on passing from $H_2NCOCONH_2$ (109 kJ mol^{-1}) (four intermolecular H bonds) to $CH_3HNCOCONHCH_3$ (83 kJ mol^{-1}) (two intermolecular H bonds) to $(CH_3)_2NCOCON(CH_3)_2$ (70 kJ mol^{-1}) (zero intermolecular H bonds) (Figure 7B).

The number of intermolecular interactions is very important. By comparing $C_3H_7HNCOCONHC_3H_7$ (mm 172) and HOC_2H_4-$HNCOCONHC_2H_4OH$ (mm 176), we find that the propyl derivative exhibits only two and the hydroxyethyl derivative exhibits only four intermolecular interactions (Figure 8).[48]

By comparing DMO (VII) $\Delta_{total}H^* = 83$, DMMTO (XV) $\Delta_{total}H^* = 82$, and DMDTO (XIV) $\Delta_{total}H^* = 79$, we also can

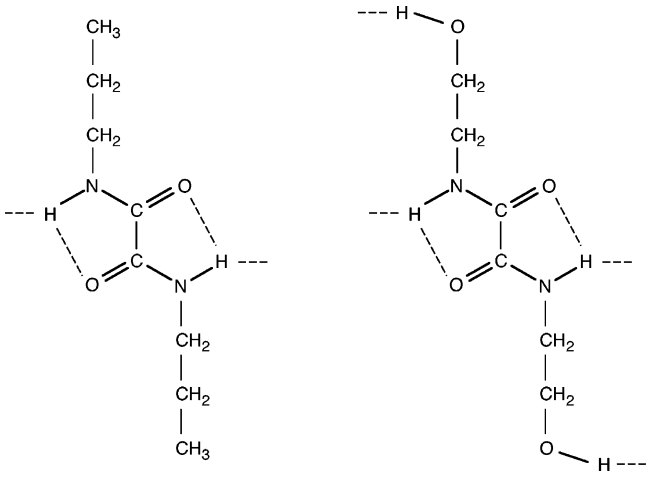

Figure 8. Intermolecular hydrogen bonds in DPO and DHEO.

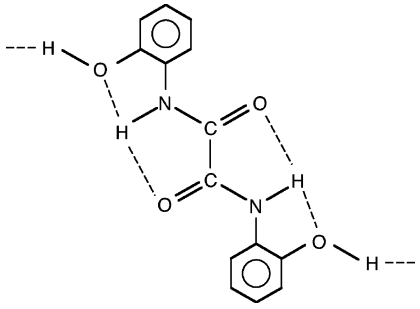

Figure 9. Geometry and hydrogen bonding in D2HPO.

TABLE 10: Comparison of Different Hydroxyphenyloxamides[a]

		D_2HPO	D_3HPO	D_4HPO
solid-state IR spectra				
νNH	25 °C	3356	3307	3295
	−196 °C	3356	3299	3286
νOH	25 °C	3311	3340	3394
	−196 °C	3291	3320	3372
$\Delta\delta/\Delta T$ (ppm/K)	OH	5.87	4.50	4.60
	NH	0.67	5.13	4.97
$\Delta_{total}H^*$ (kJ/mol)		205	decomp.	decomp.
$T(dm/dT)_{max}$		301	335	360
no. of intermolecular associations		2	4	4

[a] ν (cm^{-1}); T(°C).

state that despite the increasing mass the $\Delta_{total}H^*$ is in large part determined by the difference in the strength of the intermolecular interactions.

5. Hydroxyphenyl Oxamides. F. J. Martinez-Martinez[17] concluded from an NMR and X-ray diffraction study that in *N*,*N*′-bis(2-hydroxyphenyl)oxamide (D_2HPO) three-center intramolecular hydrogen bonding, as given in Figure 9, is comparable to that in DtBO, where the typical linear secondary amide pattern is absent. The steric influence of both the hydroxyphenyl group and the tertiary butyl group results in a very short intramolecular N···O distance (2.720 Å for DMO, 2.683 Å for DtBO, and 2.690 Å for D_2HPO[17]). We also studied the solid-state spectra and the thermal properties of the *N*-*N*′-bis-3(D_3HPO) and *N*,*N*′-bis(4-hydroxyphenyl)oxamides (D_4-HPO). The data are gathered in Table 10.

Figure 10 shows the 3500−3100-cm^{-1} region for the νNH and νOH modes of D_2HPO and D_4HPO in the solid state at different temperatures.

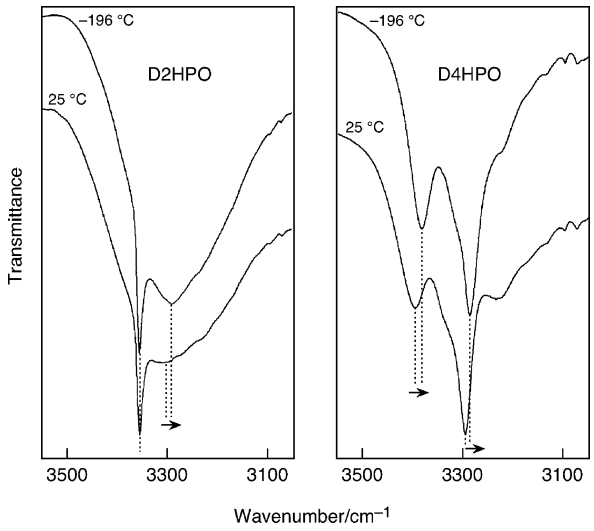

Figure 10. Solid-state spectra at different temperatures for the νNH and νOH modes in D2HPO and D4HPO.

The νNH mode in D_2HPO is not shifted at lower temperature, indicating strong intramolecular interactions; these interactions are confirmed by NH $\Delta\delta/\Delta T = 0.67$ ppm/K. The NH modes of D_3HPO and D_4HPO clearly show intermolecular associations. The OH groups for the three compounds are all intermolecularly associated, as can be learned from the vibrational and NMR data.

For D_2HPO we could very well calculate the $\Delta_{total}H^*$, whereas for D_3HPO and D_4HPO, the compounds decompose before subliming because of the four strong intermolecular interactions.

Conclusions

Two interesting series of molecules with changing hydrogen bond character have been studied by several techniques. All of the results indicate the same trend, and the results can all be regarded as substantial contributions in this study. It is also remarkable that the enthalpy data as listed in Table 8 can be interpreted only as a function of the nature of the hydrogen bonding.

The article explains why DtBO and D_2HPO do not exhibit the typical linear peptide structure due to the strong intramolecular hydrogen bonding in these molecules. The fact that $tC_4H_9HNCSCSNHtC_4H_9$ cannot be prepared, either from DTO + $tBNH_2$ or from refluxing $tC_4H_9HNCOCONHtC_4H_9$ with P_2S_5, can be explained by assuming very strong intramolecular N−H···S hydrogen bonds, resulting in the formation of H_2S during the process.

Acknowledgment. We thank Greta Thijs for technical assistance.

References and Notes

(1) Gutman, V. *The Donor:Acceptor Approach to Molecular Interactions*; Plenum Press: New York, 1978.
(2) Zefirov, Yu. V. *Crystallogr. Rep.* **1998**, *43*, 2, 278.
(3) Slootmaekers, B.; Desseyn, H. O. *Appl. Spectrosc.* **1991**, *45*, 1, 118.
(4) Herrebout, W. A.; Clou, K.; Desseyn, H. O. *J. Phys. Chem. A* **2001**, *105*, 4865.
(5) Desseyn, H. O.; Clou, K.; Keuleers, R.; Miao, R.; Van Doren, V. E.; Blaton, N. *Spectrochim. Acta, Part A* **2001**, *57*, 231.
(6) Kopple, K. D.; Onishi, M.; Go, A. *J. Am. Chem. Soc.* **1969**, *91*, 4262
(7) Onishi, M.; Urry, D. W. *Biochem. Biophys. Res. Commun.* **1969**, *36*, 194.
(8) Llinas, M.; Klein, M. P. *J. Am. Chem. Soc.* **1975**, *97*, 4731.

(9) Baxter, N. J.; Williamsom, M. P. *J. Biomol. NMR* **1997**, *9*, 359.
(10) Andersen, N. H.; Chen, C.; Marschner, T. M.; Frystek, R. R., Jr.; Bollolino, D. A. *Biochemistry* **1992**, *31*, 1280.
(11) Andersen, N. H.; Neigh, J. W.; Harris, S. M.; Lee, G. M.; Lin, Z.; Tong, H. *J. Am. Chem. Soc.* **1997**, *119*, 8547.
(12) Rothemund, S.; Weisshoff, H.; Beyermann, M.; Krause, E.; Biernert, M.; Mügge, C.; Sykes, B. D.; Sönnichsen, F. D. *J. Biomol. NMR* **1996**, *8*, 93.
(13) Dyson, H. J.; Rance, M.; Gougthen, R. S.; Lerner, R. S.; Wright, R. E. *J. Mol. Biol.* **1988**, *201*, 161.
(14) Kessler, H. *Angew. Chem.* **1982**, *94*, 509.
(15) Hansen, P. E.; Duus, F.; Neumann, R.; Wesolowska, A.; Sosnicki, J. G.; Jagodzinski, T. S. *Pol. J. Chem.* **2000**, *74*, 409.
(16) Hansen, P. E.; Duus, F.; Bolvig, S.; Jagodzinski, T. S. *J. Mol. Struct.* **1996**, *378*, 45.
(17) Martinez-Martinez, F. J.; Padilla-Martinez, I. I.; Brito, M. A.; Geniz, E. D.; Rojas, R. C.; Saavedra, J. B. R.; Höpfl, H.; Tlahuextl, M.; Contreras, R. *J. Chem. Soc., Perkin Trans.* **1998**, *2*, 401.
(18) Rae, I. D. *Aust. J. Chem.* **1974**, *27*, 2617.
(19) Gellman, S. H.; Adams, B. R.; Dado, G. P. *J. Am. Chem. Soc.* **1990**, *112*, 460.
(20) Gellman, S. H.; Dado, G. P.; Liang, G.-B.; Adams, B. R. *J. Am. Chem. Soc.* **1991**, *113*, 1164.
(21) Liang, G.-B.; Rito, C. J.; Gellman, S. H. *J. Am. Chem. Soc.* **1992**, *114*, 4440.
(22) Liang, G.-B.; Desper, J. M.; Gellman, S. H. *J. Am. Chem. Soc.* **1993**, *115*, 925.
(23) Dado, G. P.; Gellman, S. H. *J. Am. Chem. Soc.* **1994**, *116*, 1054.
(24) Desseyn, H. O. *Pure Appl. Chem.* **1989**, *61*, 867.
(25) Aarts, A. J., Herman, M. A. *Bull. Soc. Chim. Belg.* **1977**, *86*, 757.
(26) Jeffrey, G. A. *An Introduction to Hydrogen Bonding*; University Press: Oxford, U.K., 1997.
(27) De Beukeleer, S. J. H.; Janssens, J. F.; Desseyn, H. O. *J. Therm. Anal.* **1997**, *48*, 225.
(28) Hibbert, F.; Emsley, J. *Adv. Phys. Org. Chem.* **1990**, *23*, 256.
(29) De Siraju, G. R.; Steiner, T. *The Weak Hydrogen Bonds*; University Press: Oxford, U.K., 1997.
(30) Schuster, P.; Mikenda, W. *Hydrogen Bond Research*; Springer-Verlag: Wien, Austria, 1999.
(31) Quaeyhaegens, F.; Desseyn, H. O.; Bracke, B.; Lenstra, A. T. H. *J. Mol. Struct.* **1990**, *238*, 139.
(32) Martinez-Martinez, F. J.; Ariza-Castolo, A.; Tlahuextl, H.; Tlahuextl, M.; Contreras, R. *J. Chem. Soc., Perkin Trans.* **1993**, *2*, 1481.
(33) North, A. C. T.; Phillips, D. C.; Mathews, F. S. *Acta Crystallogr., Sect. A* **1968**, *24*, 351.
(34) Altomare, A.; Cascarano, G.; Giacovazzo, C.; Guagliardi, A.; Burla, M. C.; Polidori, G.; Camalli, M. *J. Appl. Crystallogr.* **1994**, *27*, 435.
(35) Sheldrick, G. M.; *Shelxl 97: Program for the Refinement of Crystal Structures*; University of Göttingen: Göttingen, Germany, 1997.
(36) Klaska, K. H.; Jarchow, O.; Scham, W.; Widjaja, H.; Voss, J.; Schmail, H. N. *J. Chem. Res.* **1980**, 1643.
(37) Frisch, M. J.; Trucks, G. W.; Schlegel, H. B.; Scuseria, G. E.; Robb, M. A.; Cheeseman, J. R.; Zakrzewski, V. G.; Montgomery, J. A., Jr.; Stratmann, R. E.; Burant, J. C.; Dapprich, S.; Millam, J. M.; Daniels, A. D.; Kudin, K. N.; Strain, M. C.; Farkas, O.; Tomasi, J.; Barone, V.; Cossi, M.; Cammi, R.; Mennucci, B.; Pomelli, C.; Adamo, C.; Clifford, S.; Ochterski, J.; Petersson, G. A.; Ayala, P. Y.; Cui, Q.; Morokuma, K.; Malick, D. K.; Rabuck, A. D.; Raghavachari, K.; Foresman, J. B.; Cioslowski, J.; Ortiz, J. V.; Stefanov, B. B.; Liu, G.; Liashenko, A.; Piskorz, P.; Komaromi, I.; Gomperts, R.; Martin, R. L.; Fox, D. J.; Keith, T.; Al-Laham, M. A.; Peng, C. Y.; Nanayakkara, A.; Gonzalez, C.; Challacombe, M.; Gill, P. M. W.; Johnson, B. G.; Chen, W.; Wong, M. W.; Andres, J. L.; Head-Gordon, M.; Replogle, E. S.; Pople, J. A. *Gaussian 98*, revision A.5; Gaussian, Inc.: Pittsburgh, PA, 1998.
(38) Becke, A. D. *J. Chem. Phys.* **1993**, *98*, 5648.
(39) Lee, C.; Yang, W.; Parr, R. G. *Phys. Rev. B* **1988**, *37*, 785.
(40) Hibbert, F.; Emsley, J. *Adv. Phys. Org. Chem.* **1990**, *26*, 255.
(41) Geboes, P.; Hofmans H.; Desseyn, H.; Dommisse R., Lenstra A.; Sanni S.; Smit J.; Beurskens P. *Spectrochim. Acta, Part A* **1987**, *43*, 35.
(42) Vinogradov, S. N.; Linell, R. H. *Hydrogen Bonding*; Van Nostrand: New York, 1971.
(43) Ghosh, P. N. *J. Phys. C: Solid State Phys.* **1977**, *10*, 4421.
(44) Desseyn, H. O.; Aarts, A. J.; Esmans, E.; Herman, M. A. *Spectrochim. Acta, Part A* **1979**, *35*, 1203.
(45) Ovchinnikov, Y. K.; Ivanov, V. T. *Tetrahedron* **1975**, *31*, 2177.
(46) Bara, Y. A.; Friedrich, A.; Kessler, H.; Molter, M. *Chem. Ber.* **1978**, *111*, 1045.
(47) Kessler, H.; Hölzemann, G. *Liebigs Ann. Chem.* **1981**, 2028.
(48) Wolfs, I.; Desseyn, H. O.; Perlepes, S. P. *Spectrochim. Acta, Part A* **1994**, *50*, 1141.